WESTINGHOUSE PROPRIETARY CLASS 3

WCAP-10902

CUSTOMER DESIGNATED DISTRIBUTION

PLANT SPECIFIC NEUTRON FLUENCE EVALUATION FOR ZION UNITS 1 AND 2

S. L. Anderson

WORK PERFORMED FOR COMMONWEALTH EDISON COMPANY

AUGUST 1985

Approved: 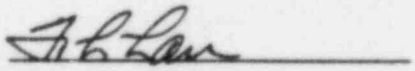

F. L. Lau, Manager
Radiation and Systems
Analysis

WESTINGHOUSE ELECTRIC CORPORATION
NUCLEAR ENERGY SYSTEMS
P. O. BOX 355
PITTSBURGH, PENNSYLVANIA 15230

EXECUTIVE SUMMARY

The Westinghouse Adjoint Flux tool has been used to assess the effects that past, present, and projected fuel management strategies have on fast neutron exposure levels in the Zion Unit 1 and 2 reactor pressure vessels.

In regard to the low leakage fuel management already in place at the Zion plants, the plant specific evaluations have demonstrated that, for the low leakage case, the average peak fast neutron flux at the 45° azimuthal position has been reduced by about 35% at Unit 1 and 25% at Unit 2 relative to that existing prior to implementation of low leakage. Other vessel locations have been impacted to a lesser degree. Since significant deviations from the low leakage scheme already in place will affect the exposure projections beyond the current operating cycle, future loading patterns should be evaluated, as they evolve, to determine their potential impact on the various considerations related to the reactor vessel.

The magnitude of the neutron flux at the surveillance capsule locations and the lead factors relating capsule exposure to maximum vessel exposure have been impacted by the in-place low leakage loading. Capsule withdrawal schedules should be adjusted based on the plant specific information given in this report and factoring in future changes in fuel management strategy. Excellent agreement has also been demonstrated between measured data from three withdrawn surveillance capsules and the values calculated using the adjoint flux tool.

The fuel management strategies employed to date essentially have had no impact on the schedule of applicability for the heatup and cooldown curves currently in the Zion Unit 1 and 2 technical specifications used for plant operations.

TABLE OF CONTENTS

LIST OF TABLES

LIST OF TABLES (Continued)

LIST OF FIGURES

LIST OF FIGURES (Continued)

SECTION I
INTRODUCTION

The Westinghouse Adjoint Flux Program provides a cost effective tool to assess the effects that past and present core management strategies have had on neutron fluence levels in the reactor pressure vessel, along with several other considerations. This report presents the results from application of the adjoint flux program to the Zion Unit 1 and 2 reactor vessels for Commonwealth Edison Company. Both of these plants have recently operated using non-design basis core management schemes.

Section II outlines the adjoint methodology, discusses the fuel management schemes that have been used to date, and presents the neutron fluence data for both the design basis and actual core management strategies. The resulting impact of these actual fuel management schemes on the intermediate and power range excore detectors, the lead factors and removal schedules for the surveillance capsules, and the schedule of applicability for the heat-up and cooldown curves is also given.

Results of the plant specific fluence evaluations are summarized in Section III and the references for the report are provided in Section IV. Appendix A shows the core power distributions used in the neutron fluence analysis.

SECTION II

NEUTRON EXPOSURE EVALUATION

II.1 METHOD OF ANALYSIS

A plan view of the Zion Unit 1 and 2 reactor geometry at the core midplane is shown in Figure II.1-1. Since the reactor exhibits 1/8th core symmetry only a 0°-45° sector is depicted. Eight irradiation capsules attached to the thermal shield are included in the design to constitute the reactor vessel surveillance program. Four capsules are located 180° symmetrically at azimuthal positions of 4° and 40° from the reactor core cardinal axes as shown in Figure II.1-1.

A plan view of a single surveillance capsule attached to the thermal shield is shown in Figure II.1-2. The stainless steel specimen container is 1-inch square and approximately 38 inches in height. The containers are positioned axially such that the specimens are centered on the core midplane, thus spanning the central 3.17 feet of the 12-foot high reactor core.

In performing the fast neutron exposure evaluations for the reactor geometry shown in Figures II.1-1 and II.1-2, two sets of transport calculations were carried out. The first, a single computation in the conventional forward mode, was utilized to provide baseline data derived from a design basis core power distribution against which cycle by cycle plant specific calculations can be compared. The second set of calculations consisted of a series of adjoint analyses relating the response of interest at several selected locations within the reactor geometry to the power distributions in the reactor core. These adjoint importance functions when combined with cycle specific core power distributions yield the plant specific exposure data for each operating fuel cycle.

Figure II. 1-1
ZION REACTOR GEOMETRY

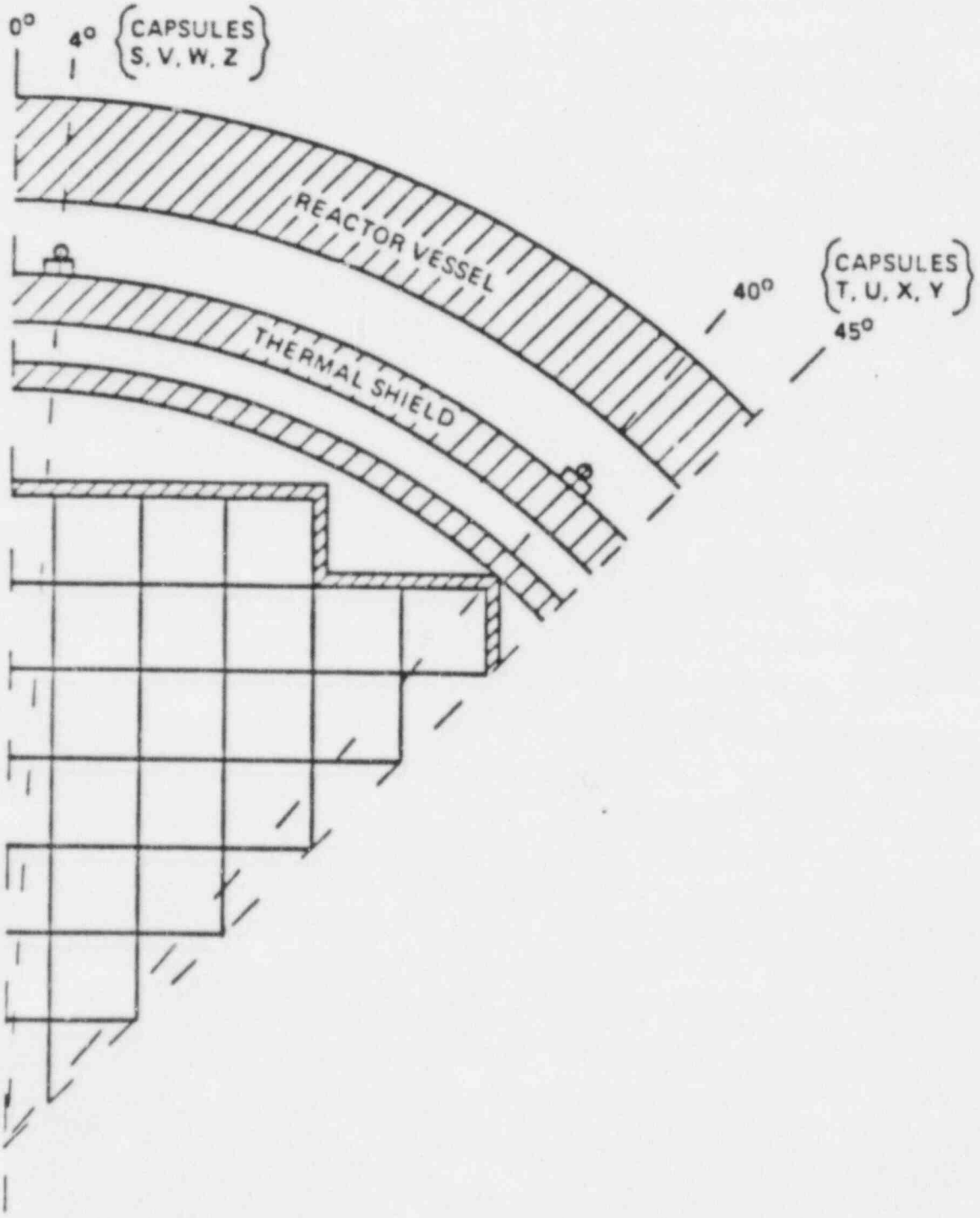

Figure II. 1-2
SURVEILLANCE CAPSULE GEOMETRY

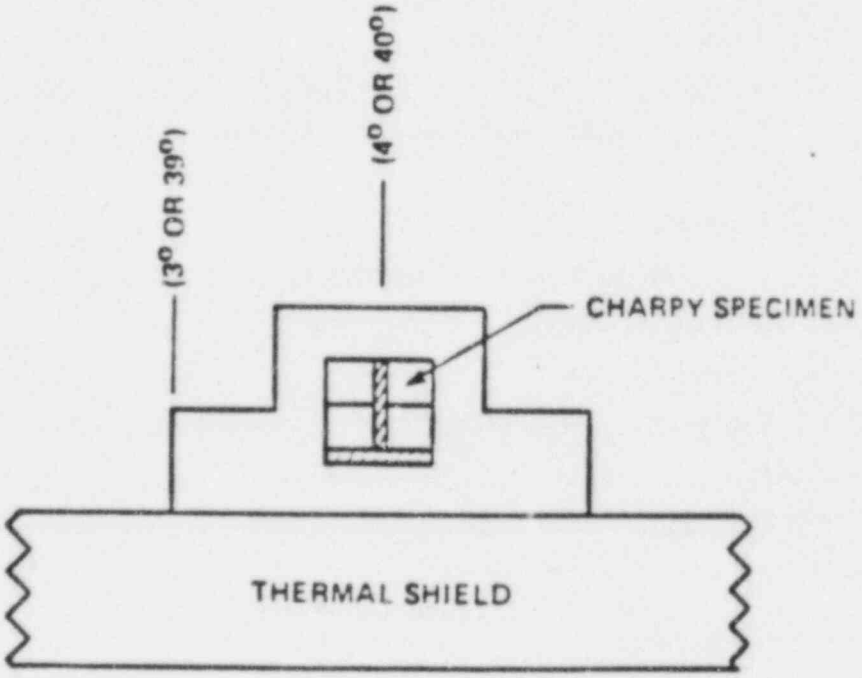

The forward transport calculation was carried out in R,θ geometry using the DOT discrete ordinates code [1] and the SAILOR cross-section library [2]. The SAILOR library is a 47 group, ENDF-BIV based data set produced specifically for light water reactor applications. Anisotropic scattering is treated with a P_3 expansion of the cross-sections.

The design basis core power distribution utilized in the forward analysis was derived from statistical studies of long-term operation of Westinghouse 4-loop plants. Inherent in the development of this design basis core power distribution is the use of an out-in fuel management strategy; i.e., fresh fuel on the core periphery. Furthermore, for the peripheral fuel assemblies, a 2σ uncertainty derived from the statistical evaluation of plant to plant and cycle to cycle variations in peripheral power was used. Since it is unlikely that a single reactor would have a power distribution at the nominal +2σ level for a large number of fuel cycles, the use of this design basis distribution is expected to yield somewhat conservative results.

The adjoint analyses were also carried out using the P_3 cross section approximation from the SAILOR library. Adjoint source locations were chosen at the center of each of the surveillance capsules as well as at positions along the inner diameter of the pressure vessel. Again, these calculations were run in R,θ geometry to provide power distribution importance functions for the exposure parameters of interest. Having the adjoint importance functions and appropriate core power distributions, the response of interest is calculated as:

$$R_{R,\theta} = \int_R \int_\theta I(R,\theta)\, F(R,\theta)\, R\, dR\, d\theta$$

where:

$R_{R,\theta}$ = Response of interest (ϕ (E > 1.0 MeV), dPa, etc.) at radius R and azimuthal angle θ.

(I (R,θ) = Adjoint importance function at radius R and azimuthal angle θ

F (R,θ) = Full power fission density at radius R and azimuthal angle θ

It should be noted that as written in the above equation, the importance function I(RΘ) represents an integral over the fission distribution so that the response of interest can be related directly to the spatial distribution of fission density within the reactor core.

Core power distributions for use in the plant specific fluence evaluations for Zion Units 1 and 2 were taken from the design of each operating cycle for the two reactors. The specific power distribution data used in the analysis is provided in Appendix A of this report. The data listed in Appendix A represents cycle averaged relative assembly powers. Therefore, the adjoint results are in terms of fuel cycle averaged neutron flux which when multiplied by the fuel cycle length yields the incremental fast neutron fluence.

The transport methodology, both forward and adjoint, using the SAILOR cross-section library has been benchmarked against the ORNL PCA facility as well as against the Westinghouse power reactor surveillance capsule data base[3]. The benchmarking studies indicate that the use of SAILOR cross-sections and generic design basis power distributions produces flux levels that tend to be conservative by from 7-22%. When plant specific power distributions are used with the adjoint importance functions, the benchmarking studies show that fluence predictions are within $\pm$ 15% of measured values at surveillance capsule locations.

II.2 FAST NEUTRON FLUENCE RESULTS

Calculated fast neutron (E >1.0 MeV) exposure results for Zion Units 1 and 2 are presented in Tables II.2-1 through II.2-12 and in Figures II.2-1 through II.2-8. Data is presented at several azimuthal locations on the inner radius of the pressure vessel as well as at the center of each surveillance capsule.

In Tables II.2-1 through II.2-4 plant specific neutron flux and fluence levels at 0°, 15°, 30°, and 45° on the pressure vessel inner radius are listed for each operating cycle of Zion Unit 1. Also presented are the design basis fluence levels predicted using the generic 4-loop core power distribution at the nominal + 2σ level. Similar data for the center of surveillance capsules located at 4° and 40° are given in Tables II.2-5 and II.2-6, respectively.

In addition to the calculated data given for the surveillance capsule locations, measured fluence data from previously withdrawn surveillance capsules are also presented for comparison with analytical results. In the case of Unit 1, capsules were removed from the 40° location at the end of cycles 1, 4 and 6.

Plant specific and design basis fast neutron flux and fluence data at the inner radius of the pressure vessel are given in Tables II.2-7 through II.2-10 for each operating cycle of Zion Unit 2. As in the case of Unit 1, data are presented for the 0°, 15°, 30°, and 45° azimuthal angles. Evaluations of plant specific and design basis fluence levels at the two surveillance capsule locations are given in Tables II.2-11 and II.2-12.

For Unit 2, surveillance capsules were removed from the 40° position following cycles 1 and 4. Dosimetry evaluations from these two capsule withdrawals are also listed in Table II.2-12.

Several observations regarding the data presented in Tables II.2-1 through II.2-12 are worthy of note. These observations may be summarized as follows:

TABLE II.2-1

FAST NEUTRON (E > 1.0 MeV) EXPOSURE AT THE PRESSURE VESSEL INNER RADIUS - 0° AZIMUTHAL ANGLE

ZION UNIT 1

Cycle No.	Irradiation Time (EFPS)	Cycle Avg. Flux (n/cm^2-sec)	Cumulative Fluence (n/cm^2) Plant Specific	Design Basis
1	3.66×10^7	7.46×10^9	2.73×10^{17}	3.37×10^{17}
2	2.84×10^7	8.46×10^9	5.13×10^{17}	5.99×10^{17}
3	2.15×10^7	8.63×10^9	6.99×10^{17}	7.98×10^{17}
4	2.46×10^7	8.10×10^9	8.98×10^{17}	1.02×10^{18}
5	2.37×10^7	8.82×10^9	1.11×10^{18}	1.24×10^{18}
6	2.40×10^7	8.52×10^9	1.31×10^{18}	1.46×10^{18}
7	2.68×10^7	8.66×10^9	1.54×10^{18}	1.71×10^{18}

Note: Design Basis $\phi = 9.22 \times 10^9$ n/cm^2 - sec

TABLE II.2-2

FAST NEUTRON (E > 1.0 MeV) EXPOSURE AT THE PRESSURE VESSEL INNER RADIUS - 15° AZIMUTHAL ANGLE

ZION UNIT 1

Cycle No.	Irradiation Time (EFPS)	Cycle Avg. Flux (n/cm^2-sec)	Cumulative Fluence (n/cm^2) Plant Specific	Design Basis
1	3.66×10^7	1.16×10^{10}	4.82×10^{17}	5.27×10^{17}
2	2.84×10^7	1.32×10^{10}	8.57×10^{17}	9.36×10^{17}
3	2.15×10^7	1.35×10^{10}	1.15×10^{18}	1.25×10^{18}
4	2.46×10^7	1.29×10^{10}	1.46×10^{18}	1.60×10^{18}
5	2.37×10^7	1.45×10^{10}	1.81×10^{18}	1.94×10^{18}
6	2.40×10^7	1.41×10^{10}	2.15×10^{18}	2.29×10^{18}
7	2.68×10^7	1.19×10^{10}	2.47×10^{18}	2.67×10^{18}

Note: Design Basis $\phi = 1.44 \times 10^{10}$ n/cm^2-sec

TABLE II.2-3

FAST NEUTRON (E > 1.0 MeV) EXPOSURE AT THE PRESSURE VESSEL INNER RADIUS - 30° AZIMUTHAL ANGLE

ZION UNIT 1

Cycle No.	Irradiation Time (EFPS)	Cycle Avg. Flux (n/cm^2-sec)	Cumulative Fluence (n/cm^2) Plant Specific	Design Basis
1	3.66×10^7	1.46×10^{10}	5.34×10^{17}	6.55×10^{17}
2	2.84×10^7	1.60×10^{10}	9.89×10^{17}	1.16×10^{18}
3	2.15×10^7	1.69×10^{10}	1.35×10^{18}	1.55×10^{18}
4	2.46×10^7	1.68×10^{10}	1.77×10^{18}	1.99×10^{18}
5	2.37×10^7	1.81×10^{10}	2.19×10^{18}	2.41×10^{18}
6	2.40×10^7	1.79×10^{10}	2.62×10^{18}	2.84×10^{18}
7	2.68×10^7	1.14×10^{10}	2.93×10^{18}	3.32×10^{18}

Note: Design Basis $\phi = 1.79 \times 10^{10}$ n/cm^2 - sec

TABLE II.2-4

FAST NEUTRON (E > 1.0 MeV) EXPOSURE AT THE PRESSURE VESSEL INNER RADIUS - 45° AZIMUTHAL ANGLE

ZION UNIT 1

Cycle No.	Irradiation Time (EFPS)	Cycle Avg. Flux (n/cm^2-sec)	Cumulative Fluence (n/cm^2) Plant Specific	Design Basis
1	3.66×10^7	2.18×10^{10}	7.98×10^{17}	1.01×10^{18}
2	2.84×10^7	2.35×10^{10}	1.47×10^{18}	1.80×10^{18}
3	2.15×10^7	2.64×10^{10}	2.03×10^{18}	2.40×10^{18}
4	2.46×10^7	2.63×10^{10}	2.68×10^{18}	3.08×10^{18}
5	2.37×10^7	2.68×10^{10}	3.32×10^{18}	3.73×10^{18}
6	2.40×10^7	2.81×10^{10}	3.99×10^{18}	4.40×10^{18}
7	2.68×10^7	1.63×10^{10}	4.43×10^{18}	5.14×10^{18}

Note: Design Basis $\phi = 2.77 \times 10^{10}$ n/cm^2-sec

TABLE II.2-5

FAST NEUTRON (E > 1.0 MeV) EXPOSURE AT THE 4° SURVEILLANCE CAPSULE CENTER - ZION UNIT 1

Cycle No.	Irradiation Time (EFPS)	Cycle Avg. Flux (n/cm^2-sec)	Cumulative Fluence (n/cm^2) Plant Specific	Design Basis
1	3.66×10^7	2.26×10^{10}	8.35×10^{17}	1.03×10^{18}
2	2.84×10^7	2.59×10^{10}	1.57×10^{18}	1.83×10^{18}
3	2.15×10^7	2.64×10^{10}	2.14×10^{18}	2.43×10^{18}
4	2.46×10^7	2.48×10^{10}	2.75×10^{18}	3.13×10^{18}
5	2.37×10^7	2.70×10^{10}	3.40×10^{18}	3.80×10^{18}
6	2.40×10^7	2.61×10^{10}	4.01×10^{18}	4.48×10^{18}
7	2.68×10^7	2.65×10^{10}	4.71×10^{18}	5.23×10^{18}

Note: Design Basis $\phi = 2.82 \times 10^{10}$ n/cm^2-sec

TABLE II.2-6

FAST NEUTRON (E > 1.0 MeV) EXPOSURE AT THE 40°
SURVEILLANCE CAPSULE CENTER - ZION UNIT 1

Cycle No.	Irradiation Time (EFPS)	Cycle Avg. Flux (n/cm^2-sec)	Cumulative Fluence (n/cm^2) Plant Specific	Design Basis	Capsule Data
1	3.66×10^7	6.90×10^{10}	2.53×10^{18}	3.21×10^{18}	2.73×10^{18}
2	2.84×10^7	7.44×10^{10}	4.65×10^{18}	5.70×10^{18}	
3	2.15×10^7	8.36×10^{10}	6.43×10^{18}	7.59×10^{18}	
4	2.46×10^7	8.33×10^{10}	8.49×10^{18}	9.74×10^{18}	8.64×10^{18}
5	2.37×10^7	8.49×10^{10}	1.05×10^{19}	1.18×10^{19}	
6	2.40×10^7	8.90×10^{10}	1.26×10^{19}	1.39×10^{19}	1.24×10^{19}
7	2.68×10^7	5.16×10^{10}	1.40×10^{19}	1.63×10^{19}	

Note: Design Basis $\phi = 8.77 \times 10^{10}$ n/cm^2-sec

TABLE II.2-7

FAST NEUTRON (E > 1.0 MeV) EXPOSURE AT THE PRESSURE VESSEL INNER RADIUS - 0° AZIMUTHAL ANGLE

ZION UNIT 2

Cycle No.	Irradiation Time (EFPS)	Cycle Avg. Flux (n/cm^2-sec)	Cumulative Fluence (n/cm^2) Plant Specific	Design Basis
1	3.88×10^7	7.33×10^9	2.84×10^{17}	3.58×10^{17}
2	2.40×10^7	8.99×10^9	5.00×10^{17}	5.79×10^{17}
3	2.46×10^7	7.88×10^9	6.94×10^{17}	8.06×10^{17}
4	2.02×10^7	6.65×10^9	8.28×10^{17}	9.92×10^{17}
5	2.75×10^7	8.18×10^9	1.05×10^{18}	1.25×10^{18}
6	2.34×10^7	8.19×10^9	1.24×10^{18}	1.46×10^{18}
7	2.21×10^7	7.49×10^9	1.41×10^{18}	1.67×10^{18}

Note: Design Basis $\phi = 9.22 \times 10^9$ n/cm^2-sec

TABLE II.2-8

FAST NEUTRON (E > 1.0 MeV) EXPOSURE AT THE PRESSURE VESSEL INNER RADIUS - 15° AZIMUTHAL ANGLE

ZION UNIT 2

Cycle No.	Irradiation Time (EFPS)	Cycle Avg. Flux (n/cm^2-sec)	Cumulative Fluence (n/cm^2) Plant Specific	Design Basis
1	3.88×10^7	1.15×10^{10}	4.46×10^{17}	5.59×10^{17}
2	2.40×10^7	1.39×10^{10}	7.80×10^{17}	9.04×10^{17}
3	2.46×10^7	1.23×10^{10}	1.08×10^{18}	1.26×10^{18}
4	2.02×10^7	1.19×10^{10}	1.32×10^{18}	1.55×10^{18}
5	2.75×10^7	1.27×10^{10}	1.67×10^{18}	1.95×10^{18}
6	2.34×10^7	1.17×10^{10}	1.95×10^{18}	2.28×10^{18}
7	2.21×10^7	1.11×10^{10}	2.19×10^{18}	2.60×10^{18}

Note: Design Basis $\phi = 1.44 \times 10^{10}$ n/cm^2-sec

TABLE II.2-9

FAST NEUTRON (E > 1.0 MeV) EXPOSURE AT THE PRESSURE VESSEL INNER RADIUS - 30° AZIMUTHAL ANGLE

ZION UNIT 2

Cycle No.	Irradiation Time (EFPS)	Cycle Avg. Flux (n/cm^2-sec)	Cumulative Fluence (n/cm^2) Plant Specific	Design Basis
1	3.88×10^7	1.42×10^{10}	5.51×10^{17}	6.95×10^{17}
2	2.40×10^7	1.63×10^{10}	9.42×10^{17}	1.12×10^{18}
3	2.46×10^7	1.58×10^{10}	1.33×10^{18}	1.56×10^{18}
4	2.02×10^7	1.64×10^{10}	1.66×10^{18}	1.93×10^{18}
5	2.75×10^7	1.61×10^{10}	2.10×10^{18}	2.42×10^{18}
6	2.34×10^7	1.24×10^{10}	2.40×10^{18}	2.84×10^{18}
7	2.21×10^7	1.26×10^{10}	2.67×10^{18}	3.23×10^{18}

Note: Design Basis $\phi = 1.79 \times 10^{10}$ n/cm^2-sec

TABLE II.2-10

FAST NEUTRON (E > 1.0 MeV) EXPOSURE AT THE PRESSURE VESSEL INNER RADIUS - 45° AZIMUTHAL ANGLE

ZION UNIT 2

Cycle No.	Irradiation Time (EFPS)	Cycle Avg. Flux (n/cm^2-sec)	Cumulative Fluence (n/cm^2) Plant Specific	Design Basis
1	3.88×10^7	2.09×10^{10}	8.11×10^{17}	1.07×10^{18}
2	2.40×10^7	2.37×10^{10}	1.38×10^{18}	1.74×10^{18}
3	2.46×10^7	2.50×10^{10}	1.99×10^{18}	2.42×10^{18}
4	2.02×10^7	2.70×10^{10}	2.54×10^{18}	2.98×10^{18}
5	2.75×10^7	2.64×10^{10}	3.27×10^{18}	3.74×10^{18}
6	2.34×10^7	1.72×10^{10}	3.67×10^{18}	4.39×10^{18}
7	2.21×10^7	1.82×10^{10}	4.07×10^{18}	5.00×10^{18}

Note: Design Basis $\phi = 2.77 \times 10^{10}$ n/cm^2-sec

TABLE II.2-11

FAST NEUTRON (E > 1.0 MeV) EXPOSURE AT THE 4° SURVEILLANCE CAPSULE CENTER - ZION UNIT 2

Cycle No.	Irradiation Time (EFPS)	Cycle Avg. Flux (n/cm^2-sec)	Cumulative Fluence (n/cm^2) Plant Specific	Design Basis
1	3.88×10^7	2.24×10^{10}	8.69×10^{17}	1.09×10^{18}
2	2.40×10^7	2.75×10^{10}	1.53×10^{18}	1.77×10^{18}
3	2.46×10^7	2.41×10^{10}	2.12×10^{18}	2.46×10^{18}
4	2.02×10^7	2.03×10^{10}	2.53×10^{18}	3.03×10^{18}
5	2.75×10^7	2.50×10^{10}	3.21×10^{18}	3.81×10^{18}
6	2.34×10^7	2.50×10^{10}	3.79×10^{18}	4.47×10^{18}
7	2.21×10^7	2.29×10^{10}	4.31×10^{18}	5.09×10^{18}

Note: Design Basis $\phi = 2.82 \times 10^{10}$ n/cm^2-sec

TABLE II.2-12

FAST NEUTRON (E > 1.0 MeV) EXPOSURE AT THE 40° SURVEILLANCE CAPSULE CENTER - ZION UNIT 2

Cycle No.	Irradiation Time (EFPS)	Cycle Avg. Flux (n/cm^2-sec)	Cumulative Fluence (n/cm^2) Plant Specific	Design Basis	Capsule Data
1	3.88×10^7	6.62×10^{10}	2.57×10^{18}	3.40×10^{18}	2.70×10^{18}
2	2.40×10^7	7.50×10^{10}	4.37×10^{18}	5.51×10^{18}	
3	2.46×10^7	7.92×10^{10}	6.30×10^{18}	7.66×10^{18}	
4	2.02×10^7	8.55×10^{10}	8.04×10^{18}	9.44×10^{18}	8.49×10^{18}
5	2.75×10^7	8.36×10^{10}	1.04×10^{19}	1.18×10^{19}	
6	2.34×10^7	5.45×10^{10}	1.16×10^{19}	1.39×10^{19}	
7	2.21×10^7	5.76×10^{10}	1.29×10^{19}	1.58×10^{19}	

Note: Design Basis $\phi = 8.77 \times 10^{10}$ n/cm^2-sec

Figure II. 2-1

MAXIMUM FAST NEUTRON (E>1.0 MeV) FLUENCE AT THE BELTLINE WELD LOCATIONS AS A FUNCTION OF FULL POWER OPERATING TIME

ZION UNIT 1

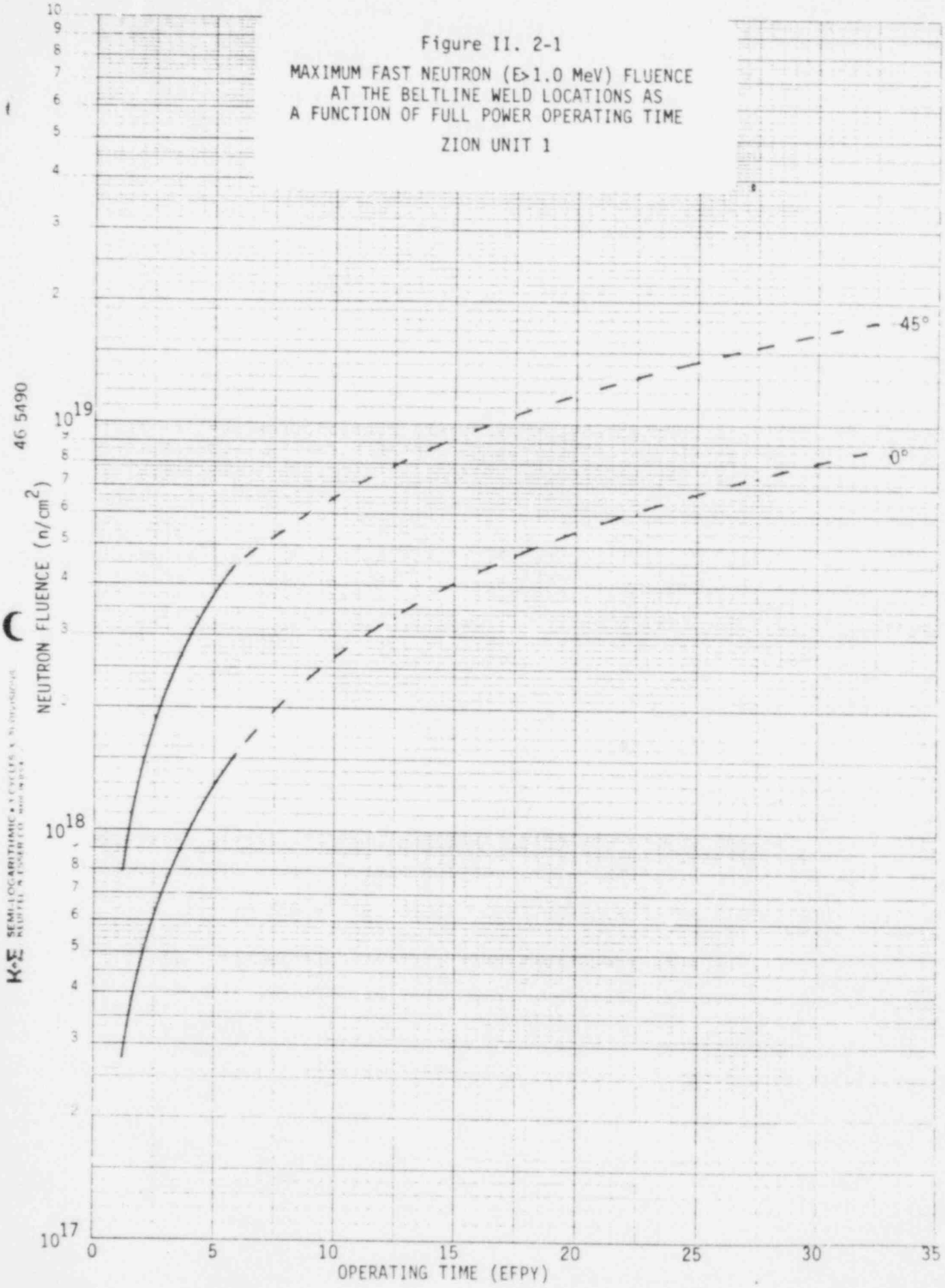

Figure II. 2-2

MAXIMUM FAST NEUTRON (E>1.0 MeV) FLUENCE AT THE CENTER OF THE SURVEILLANCE CAPSULES AS A FUNCTION OF FULL POWER OPERATING TIME

ZION UNIT 1

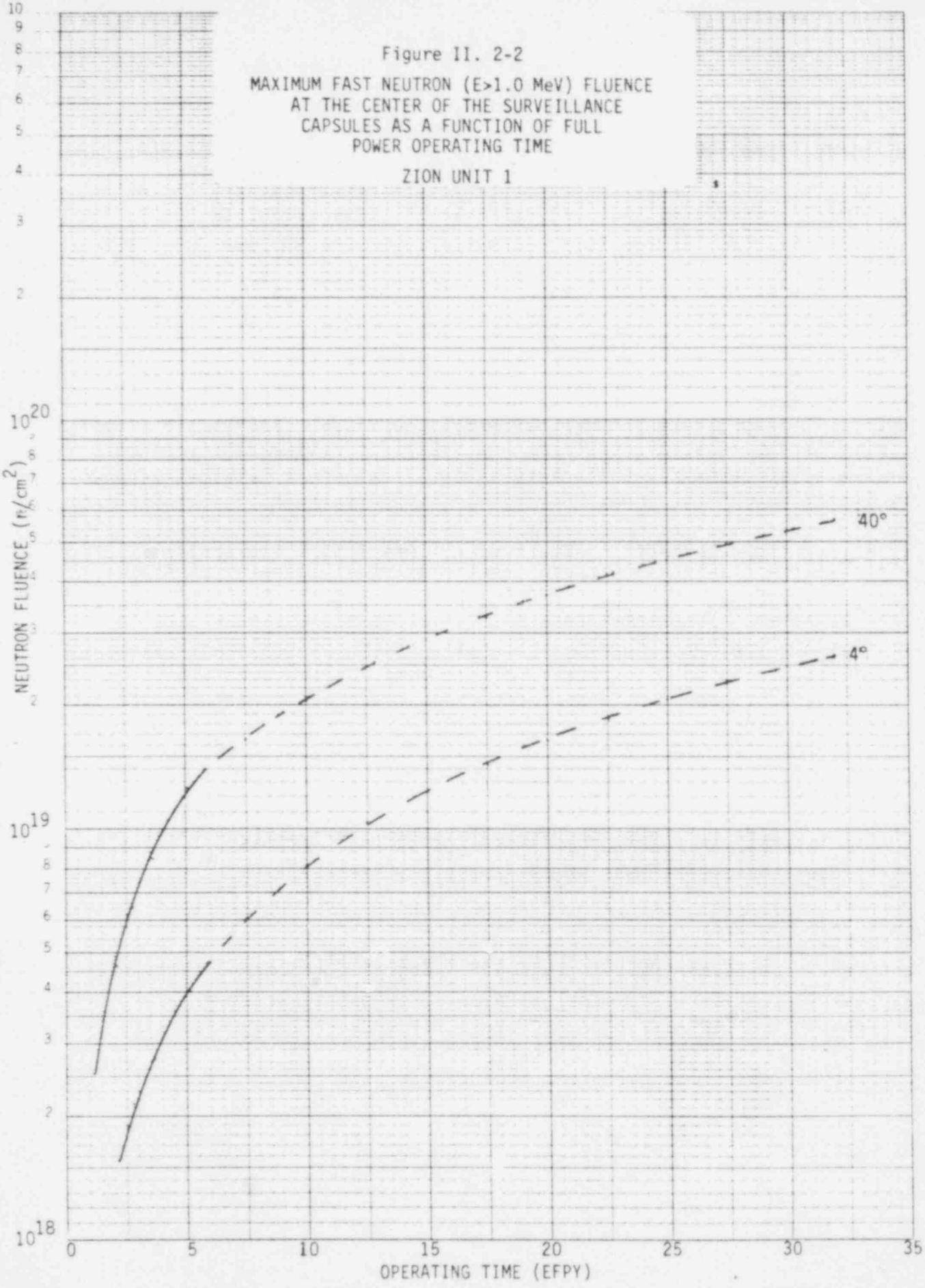

Figure II. 2-3

MAXIMUM FAST NEUTRON (E>1.0 MeV) FLUENCE AT THE BELTLINE WELD LOCATIONS AS A FUNCTION OF FULL POWER OPERATING TIME

ZION UNIT 2

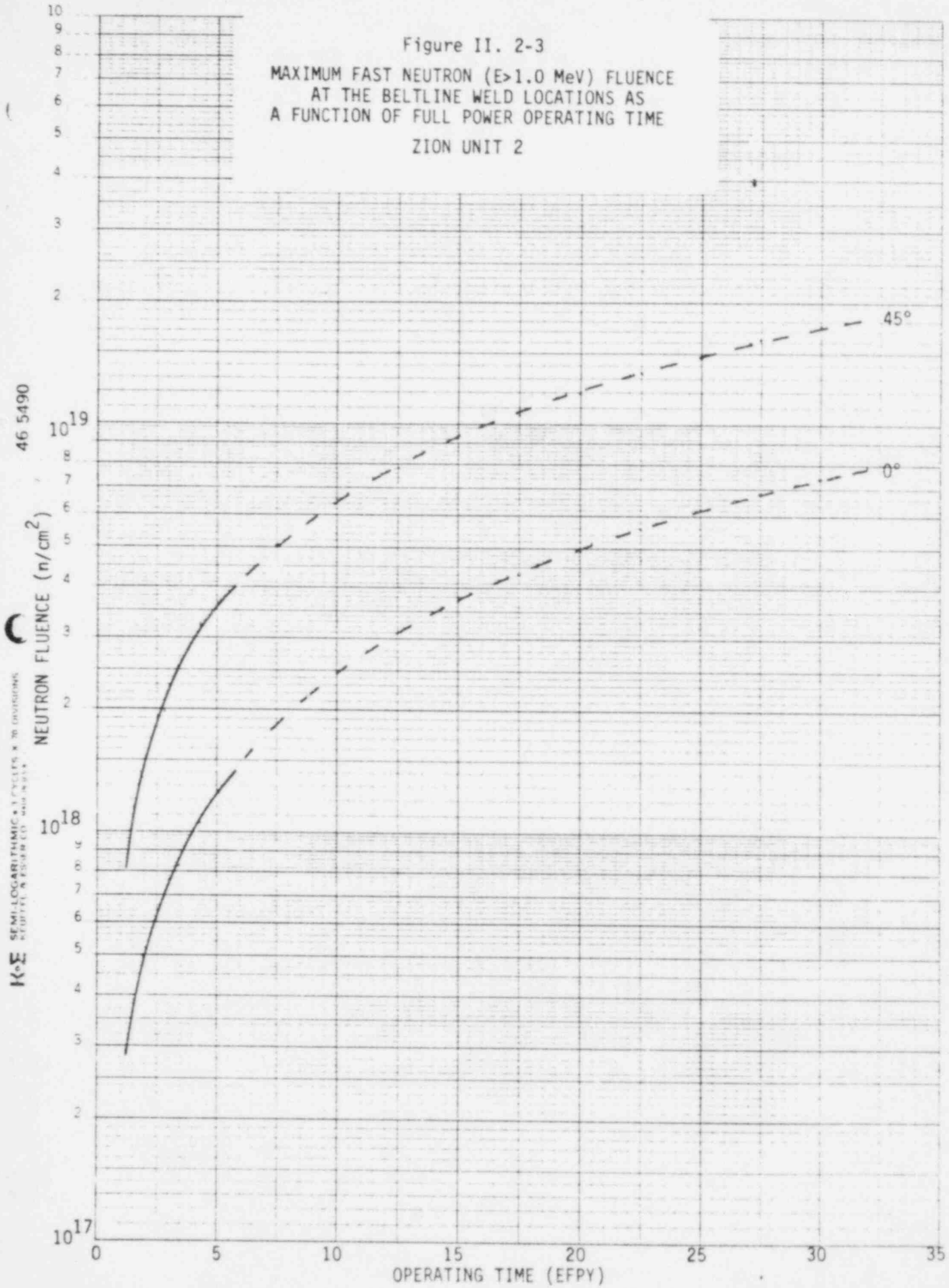

Figure II. 2-4

MAXIMUM FAST NEUTRON (E>1.0 MeV) FLUENCE AT THE CENTER OF THE SURVEILLANCE CAPSULES AS A FUNCTION OF FULL POWER OPERATING TIME

ZION UNIT 2

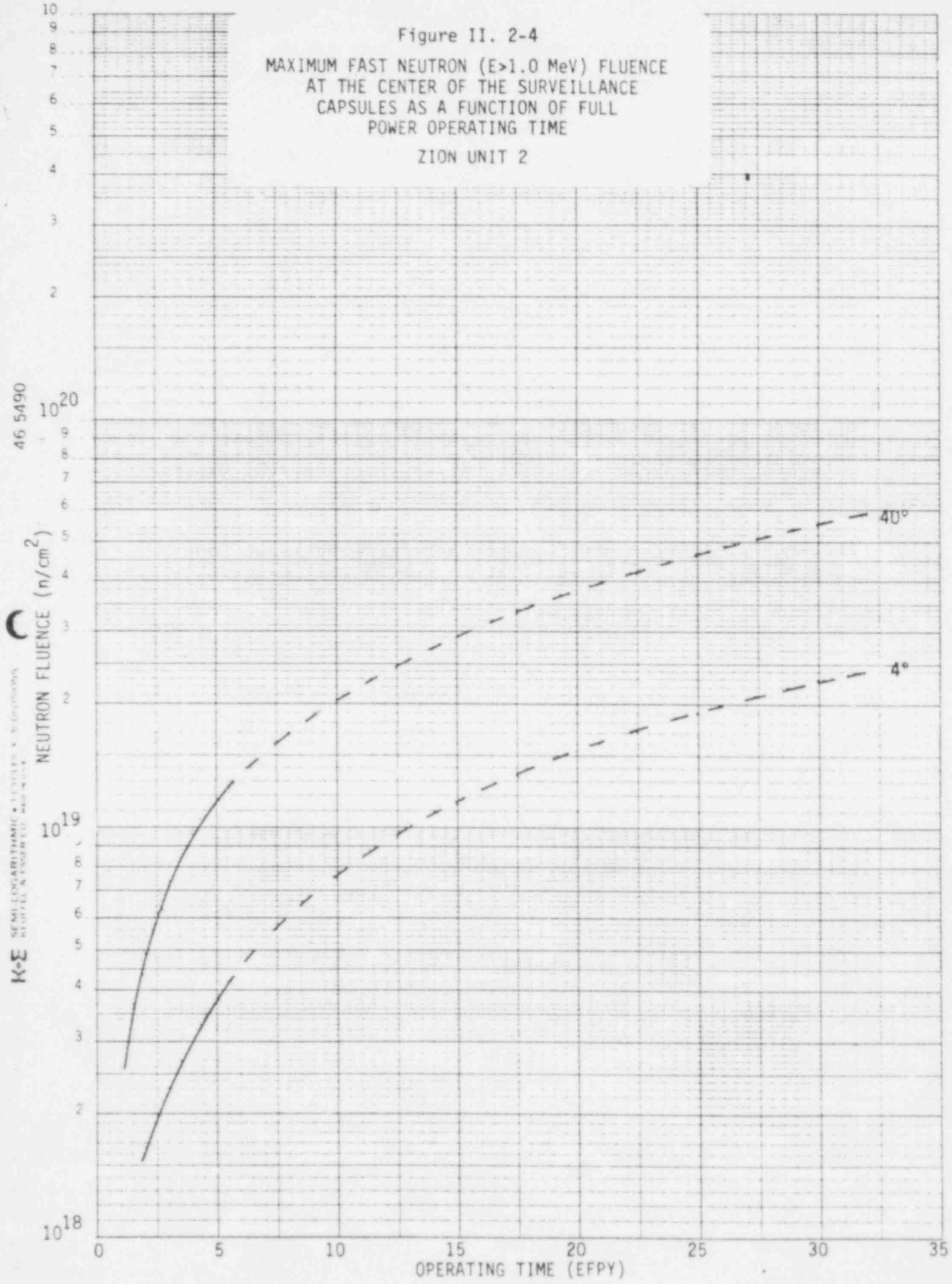

Figure II. 2-5

MAXIMUM CURRENT AND PROJECTED EOL FAST NEUTRON (E>1.0 MeV) FLUENCE AT THE PRESSURE VESSEL INNER RADIUS AS A FUNCTION OF AZIMUTHAL ANGLE

ZION UNIT 1

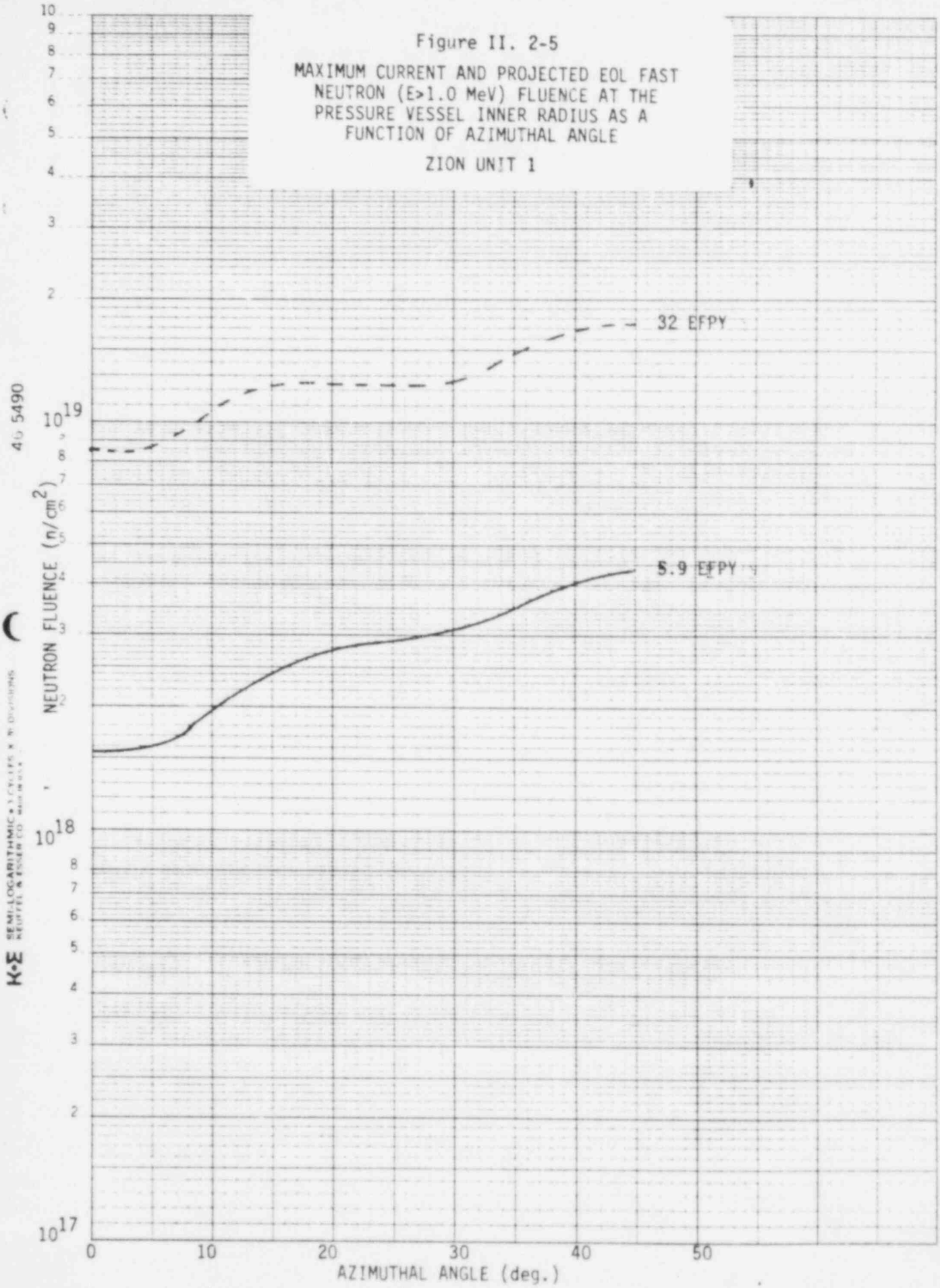

Figure II. 2-6

MAXIMUM CURRENT AND PROJECTED EOL FAST NEUTRON (E>1.0 MeV) FLUENCE AT THE PRESSURE VESSEL INNER RADIUS AS A FUNCTION OF AZIMUTHAL ANGLE

ZION UNIT 2

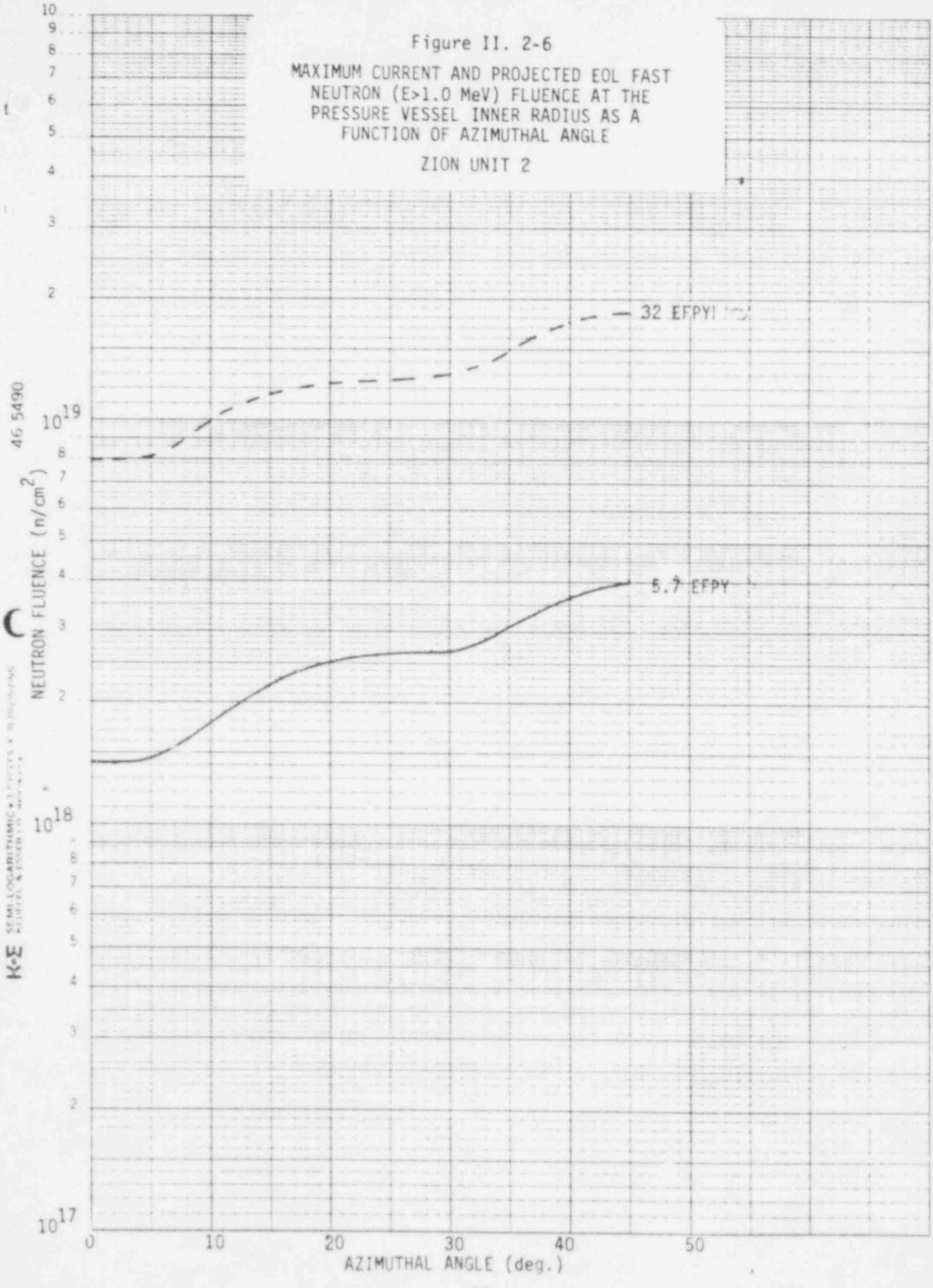

Figure II. 2-7

RELATIVE RADIAL DISTRIBUTION OF FAST NEUTRON (E>1.0 MeV) FLUX AND FLUENCE WITHIN THE PRESSURE VESSEL

ZION UNITS 1 & 2

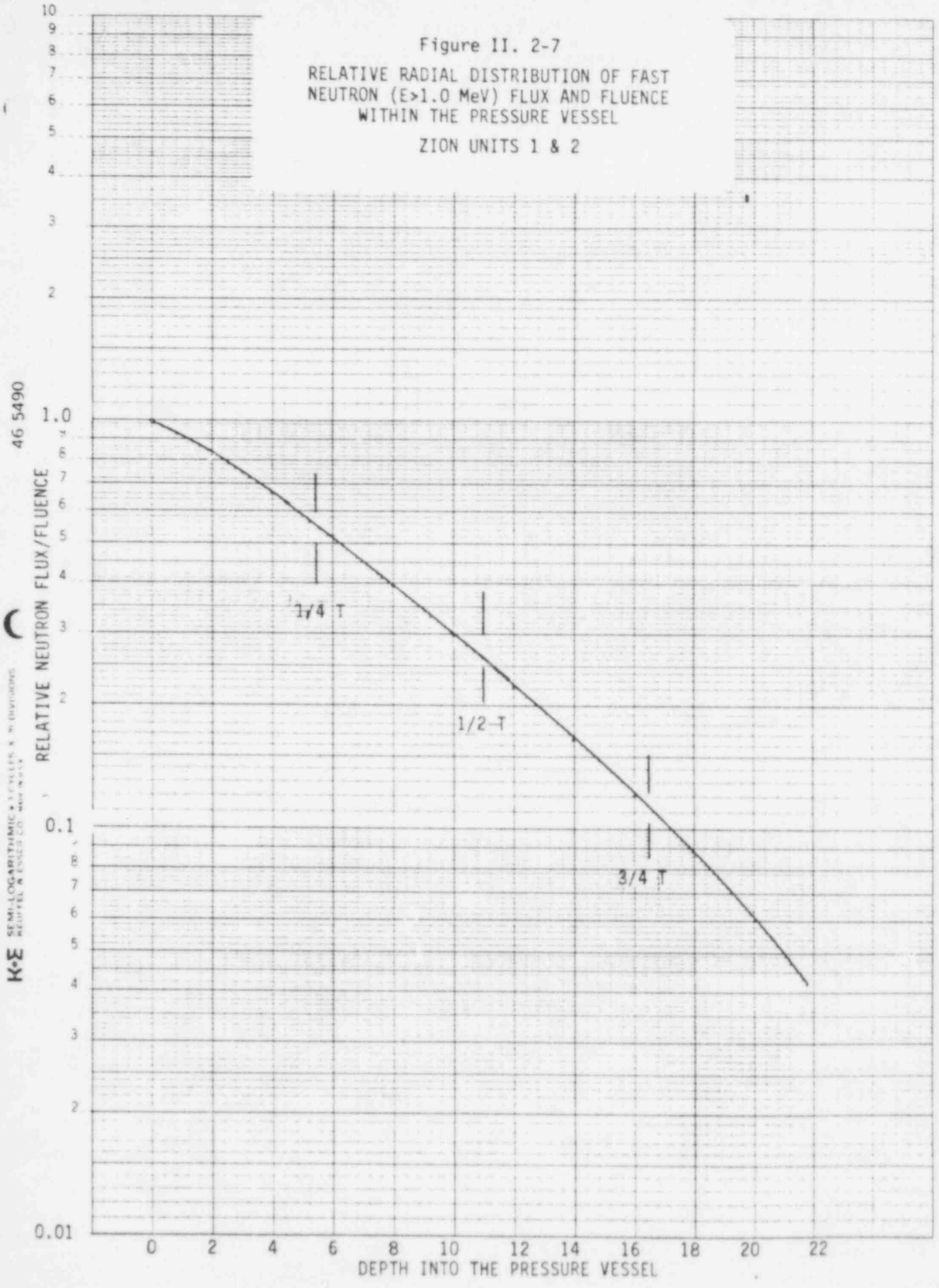

Figure II. 2-8

RELATIVE AXIAL VARIATION OF FAST NEUTRON (E>1.0 MeV) FLUX AND FLUENCE WITHIN THE PRESSURE VESSEL WALL

ZION UNITS 1 & 2

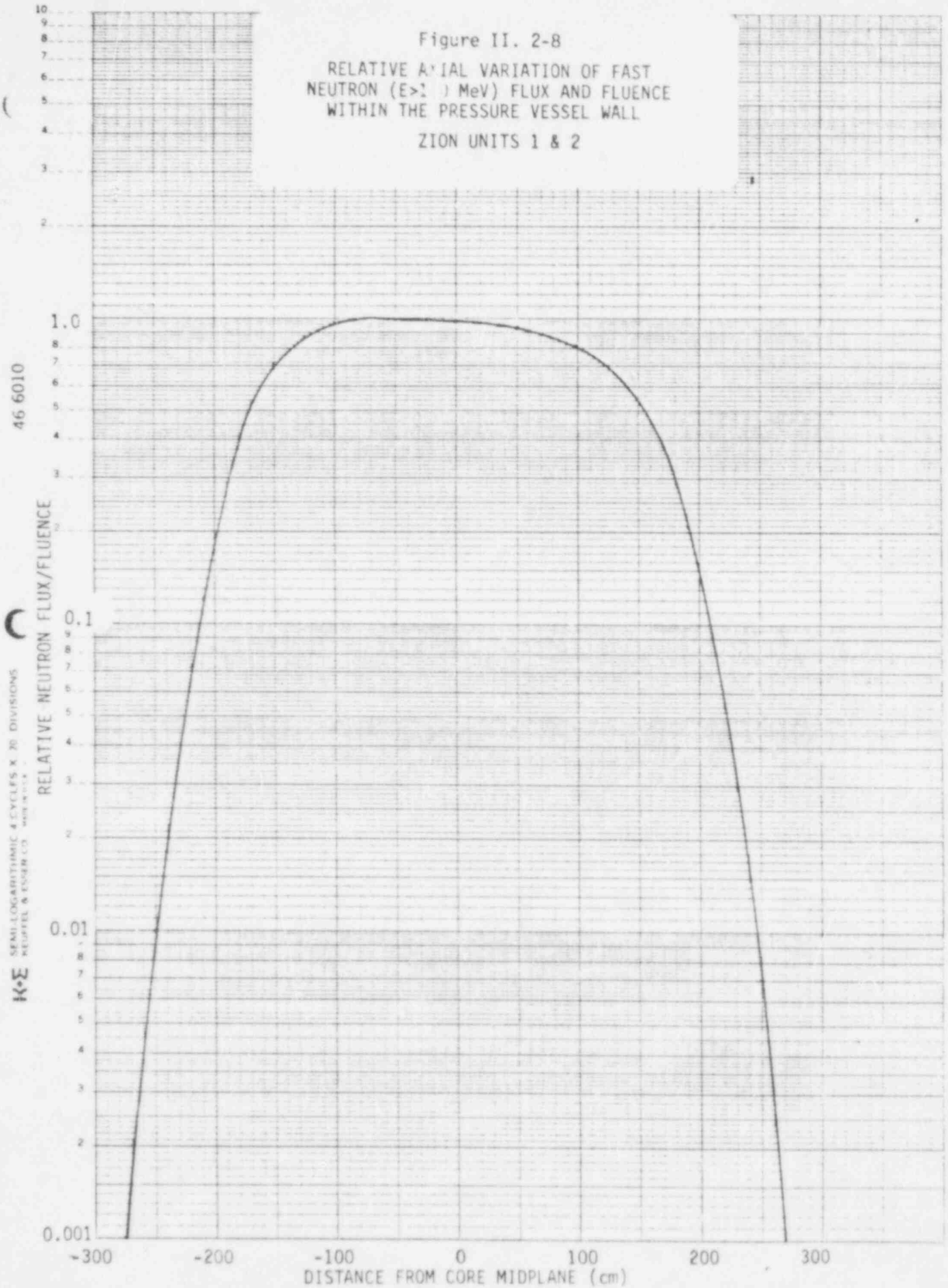

1. For both units, calculated plant specific fast neutron (E > 1.0 Mev) fluence levels at the surveillance capsule center are in excellent agreement with measured data. The maximum difference between the plant specific calculations and the measurements is less than 7%. Differences of this magnitude are well within the uncertainty of the experimental results.

2. For Unit 1, low leakage fuel management introduced following cycle 6 has reduced the peak flux on the pressure vessel by about 35%.

3. For Unit 2, low leakage fuel management introduced following cycle 5 has reduced the peak flux on the pressure vessel by about 25%. This reduction has been maintained over the last 2 operating cycles.

4. For both of the Zion reactors the maximum neutron flux incident on the pressure vessel (45° azimuthal position) during the fuel cycles using out-in fuel management (cycles 1-6 for Unit 1 and 1-5 for Unit 2) was, on the average, approximately 15% less than predictions based on the design basis core power distributions.

Graphical presentations of the plant specific fast neutron fluence at key locations on the pressure vessel as well as at the surveillance capsule center are shown in Figures II.2-1 through II.2-4 as a function of full power operating time for Zion Units 1 and 2. For both Units 1 and 2, pressure vessel data is presented for the 45° location on the circumferential weld as well as for the 0° longitudinal welds. For both reactors corresponding fluence levels at the center of 4° and 40° surveillance capsules are also depicted.

In regard to Figure II.2-1 through II.2-4, the solid portions of the fluence curves are based directly on the plant specific evaluations presented in this report. The dashed portions of these curves, however, involve a projection into the future. Since both Zion Units are committed to a consistent form of low leakage fuel management, the average neutron flux at the key locations over the low leakage fuel cycles was used for all temporal projections. In

particular, the neutron flux average over cycle 7 was used to project future fluence levels for Unit 1, while the neutron flux average over cycles 6 and 7 was employed for Unit 2.

It should be noted that implementation of a more severe low leakage pattern would act to reduce the projections of fluence at key locations. On the other hand, relaxation of the current low leakage patterns or a return to out-in fuel management would increase those projections. In any event it would be prudent to update the fluence analysis as the design of each future fuel cycle evolves.

In Figures II.2-5 and II.2-6, the azimuthal variation of maximum fast neutron ($E > 1.0$ MeV) fluence at the inner radius of the pressure vessel is presented as a function of azimuthal angle for Units 1 and 2, respectively. Data are presented for both current and projected end-of-life conditions. In Figure II.2-7, the relative radial variation of fast neutron flux and fluence within the pressure vessel wall is presented. Similar data showing the relative axial variation of fast neutron flux and fluence over the beltline region of the pressure vessel is shown in Figure II.2-8. A three-dimensional description of the fast neutron exposure of the pressure vessel wall can be constructed using the data given in Figure II.2-5 through II.2-8 along with the relation

$$\phi(R,\theta,Z) = \phi(\theta)\, F(R)\, G(Z)$$

where: $\phi(R,\theta,Z)$ = Fast neutron fluence at location R, θ, Z within the pressure vessel wall

$\phi(\theta)$ = Fast neutron fluence at azimuthal location θ on the pressure vessel inner radius from Figure II.2-5 or II.2-6

$F(R)$ = Relative fast neutron flux at depth R into the pressure vessel from Figure II.2-7

$G(Z)$ = Relative fast neutron flux at axial position Z from Figure II.2-8

Analysis has shown that the radial and axial variations within the vessel wall are relatively insensitive to the implementation of low leakage fuel management schemes. Thus, the above relationship provides a vehicle for a reasonable evaluation of fluence gradients within the vessel wall.

II.3 INFLUENCE OF AN ENERGY DEPENDENT DAMAGE MODEL

The use of fast neutron fluence (E > 1.0 MeV) to correlate measured materials properties changes to the neutron exposure of the material for light water reactor applications has traditionally been accepted for development of damage trend curves as well as for implementation of trend curve data to assess vessel condition. In recent years, however, it has been suggested that an exposure model that accounts for differences in neutron energy spectra between surveillance capsule locations and positions within the vessel wall could lead to an improvement in the uncertainties associated with damage trend curves as well as to a more accurate evaluation of damage gradients through the pressure vessel wall.

Because of this potential shift away from a threshold fluence toward an energy dependent damage function for data correlation, ASTM Standard Practice E853 "Analysis and Interpretation of Light Water Reactor Surveillance Results", recommends reporting calculated displacements per iron atom (dPa) along with fluence (E > 1.0 MeV) to provide a data base for future reference. The energy dependent dPa function to be used for this evaluation is specified in ASTM Standard Practice E693 "Characterizing Neutron Exposures in Ferritic Steels in Terms of Displacements per Atom (dPa)."

For the Zion Units 1 and 2 pressure vessels, iron atom displacement rates at each surveillance capsule location and at positions within the vessel wall have been calculated. The analysis has indicated that for a given location the ratio of $dPa/\phi(E > 1.0\ MeV)$ is insensitive to changing core power distributions. That is, while implementation of low leakage loading patterns significantly impact the magnitude and spatial distribution of the neutron field, changes in the relative neutron energy spectrum at a given location are of second order. The $dPa/\phi(E > 1.0\ MeV)$ ratios calculated for key locations in the Zion reactor geometry are given in Table II.3-1. The data in Table II.3-1 may be used in conjunction with the fast neutron fluence data provided in Section II.2 to develop distributions of dPa within the surveillance capsules and the reactor pressure vessel.

TABLE II.3-1

$dPa/\phi(E > 1.0\ MeV)$ RATIOS FOR THE ZION
UNITS 1 AND 2 REACTOR GEOMETRY

LOCATION	$dPa/\phi(E > 1.0\ MeV)$
4° CAPSULE	1.58×10^{-21}
40° CAPSULE	1.64×10^{-21}
VESSEL INNER RADIUS	1.62×10^{-21}
VESSEL 1/4 THICKNESS	1.90×10^{-21}
VESSEL 3/4 THICKNESS	3.26×10^{-21}

NOTE: RATIOS ARE IN UNITS OF
[DISPLACEMENTS PER ATOM]/[n/cm^2]

II.4 POTENTIAL IMPACT ON EXCORE NEUTRON DETECTORS

Whenever fuel management strategy changes in a way that significantly alters the power distribution around the core periphery, the potential exists to change output signals from both the power range detectors located at the 45° azimuthal position and the intermediate range detectors located at the 0° azimuth. As a result recalibration of these detectors is necessary to assure proper core power correlations. In addition, changing azimuthal distributions from cycle to cycle can effect the overlap setpoints between the intermediate and power range chambers. From an operational viewpoint it is helpful to have an a priori knowledge of the impact of a new fuel cycle design on the output of these chambers.

The data in Figures II.4-1 and II.4-2 are provided as an aid in the evaluation of the potential changes in detector response. The data as presented represents the response contribution by fuel assembly to the detector of interest. When multiplied by the relative assembly powers for a given fuel cycle design and summed over the applicable assemblies, the relative response of the detector is obtained for that particular fuel management scheme. Evaluation for two successive fuel cycles will yield the percentage change in detector response from cycle to cycle.

The data in Figures II.4-1 and II.4-2 are applicable to both of the Zion reactors.

Figure II. 4-1

RELATIVE RESPONSE OF INTERMEDIATE RANGE EXCORE
NEUTRON DETECTORS PER UNIT ASSEMBLY POWER

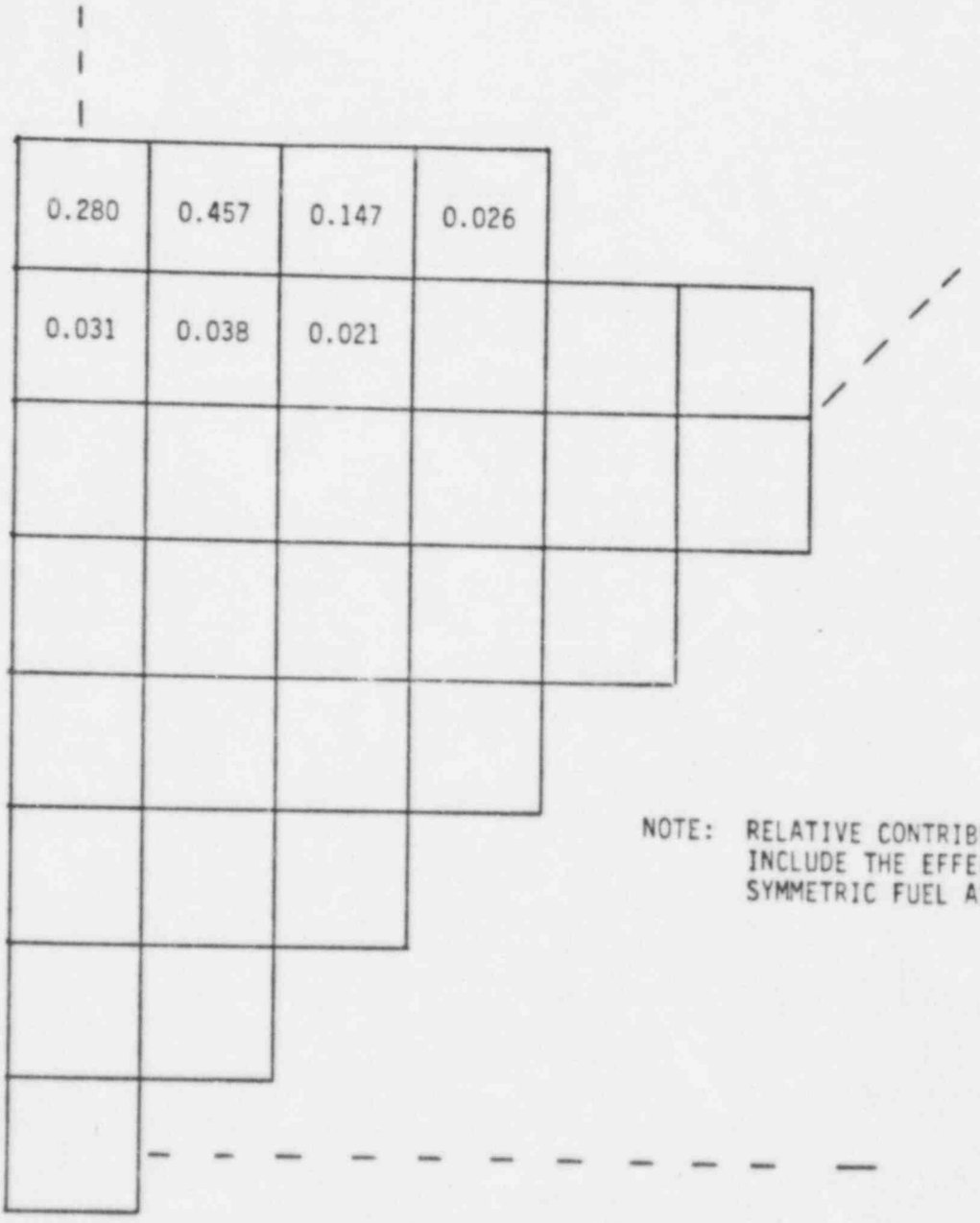

NOTE: RELATIVE CONTRIBUTIONS INCLUDE THE EFFECTS OF SYMMETRIC FUEL ASSEMBLIES

Figure II. 4-2

RELATIVE RESPONSE OF POWER RANGE EXCORE NEUTRON DETECTORS PER UNIT ASSEMBLY POWER

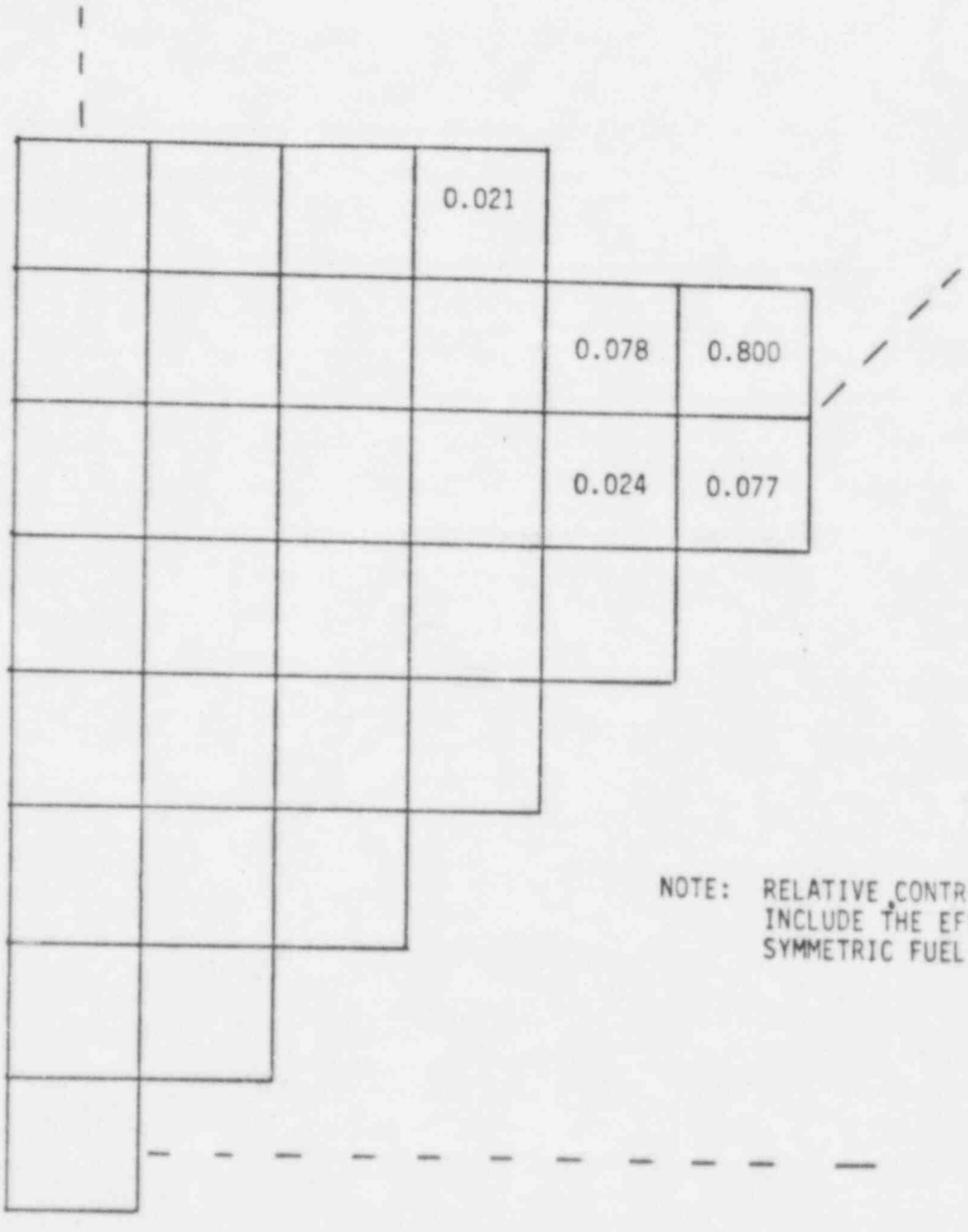

NOTE: RELATIVE CONTRIBUTIONS INCLUDE THE EFFECTS OF SYMMETRIC FUEL ASSEMBLIES

II.5 SURVEILLANCE CAPSULE WITHDRAWAL SCHEDULES

As discussed in Section II.2, plant specific fluence evaluations for the center of surveillance capsules located at 4° and 40° were presented in Figures II.2-2 and II.2-4 for Zion Units 1 and 2, respectively. The data presented on those curves represent the best available information upon which to base the future withdrawal schedules for capsules remaining in the Zion reactors.

In the past, withdrawal schedules have been based on the assumption of a constant exposure rate at the surveillance capsule center and a constant lead factor relating capsule exposure to maximum vessel exposure. With the widespread implementation of low leakage fuel management neither of these assumptions can be assumed to be universally valid. It becomes prudent, therefore, to utilize the actual anticipated capsule exposure in conjunction with appropriate materials properties data to establish capsule withdrawal dates that will provide experimental information that is of most benefit to the utility.

In evaluating future withdrawal schedules, it must be remembered that the fluence projections shown in Figures II.2-2 and II.2-4 assume continued operation with the low leakage fuel management scheme currently in place. The validity of this assumption should be verified as each new fuel cycle evolves and if significant changes occur, withdrawal schedules should be adjusted accordingly.

II.6 IMPACT ON HEATUP/COOLDOWN CURVE SCHEDULE OF APPLICABILITY

Since the fuel management schemes that have been used to date can impact the fluence pertinent to the schedule of applicability of the heatup and cooldown curves, this effect is studied in this section.

Heatup and cooldown curves were generated for the Zion Unit 1 and 2 reactor vessels in 1979, and the results were reported in References [4] and [5]. The bases for these curves relative to material properties, fluence data, and irradiation damage trend curves are also provided in References [4] and [5]. In short, the curves applicable for both reactor vessels were generated using limiting material properties for the Unit 1 circumferential weldment between the intermediate and lower shell plates. A longitudinal flaw was assumed to exist in this circumferential weld at the peak azimuthal fluence position. Both the Westinghouse and Regulatory Guide 1.99 - Rev. 1 [6] trend curves were used to determine the shift in RT_{NDT} as a result of neutron fluence accumulation. The curves were developed at 8 EFPY for both units and currently exist as such in the technical operating specifications for both units [7].

Figures II.6-1 and II.6-2 respectively show the actual and projected fluence values for the Zion Unit 1 and 2 vessels against the fluence data pertinent to the generation of the curves, i.e., the original design basis fluence curves at the 1/4 and 3/4 vessel wall thickness locations. Keeping all assumptions equal, the fuel management schemes used to date have had a minimal impact on the 8 EFPY schedule of applicability for the heatup and cooldown curves for both reactor vessels. That is, the design basis fluence associated with the 8 EFPY value is equivalent to about 8.5 EFPY for the actual and projected fluences for both Zion Units 1 and 2.

Figure II. 6-1

FAST NEUTRON (E>1.0 MeV) FLUENCE AT THE
1/4 THICKNESS AND 3/4 THICKNESS LOCATIONS
FOR HEATUP/COOLDOWN ANALYSIS

ZION UNIT 1

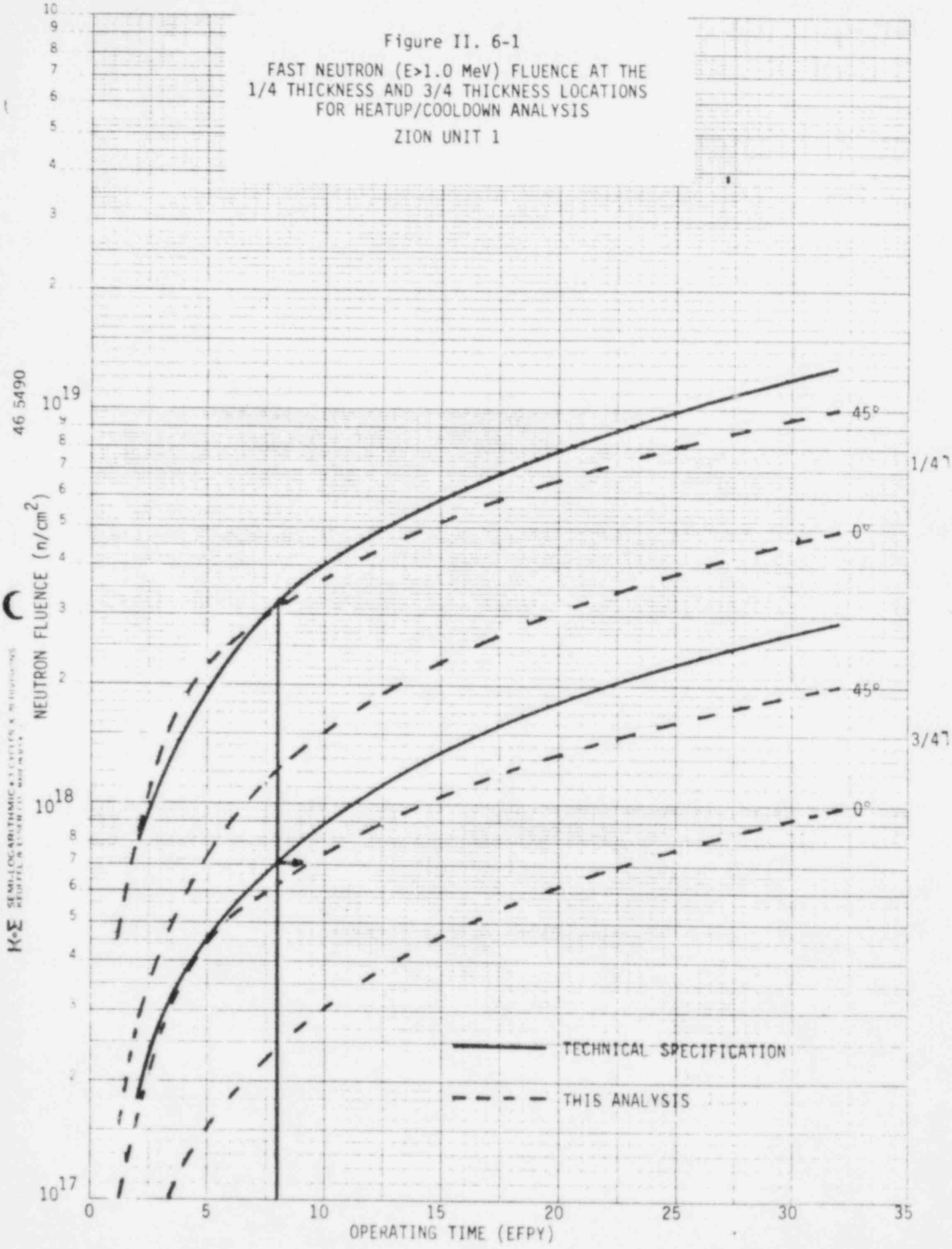

Figure II. 6-2
FAST NEUTRON (E>1.0 MeV) FLUENCE AT THE
1/4 THICKNESS AND 3/4 THICKNESS LOCATIONS
FOR HEATUP/COOLDOWN ANALYSIS

ZION UNIT 2

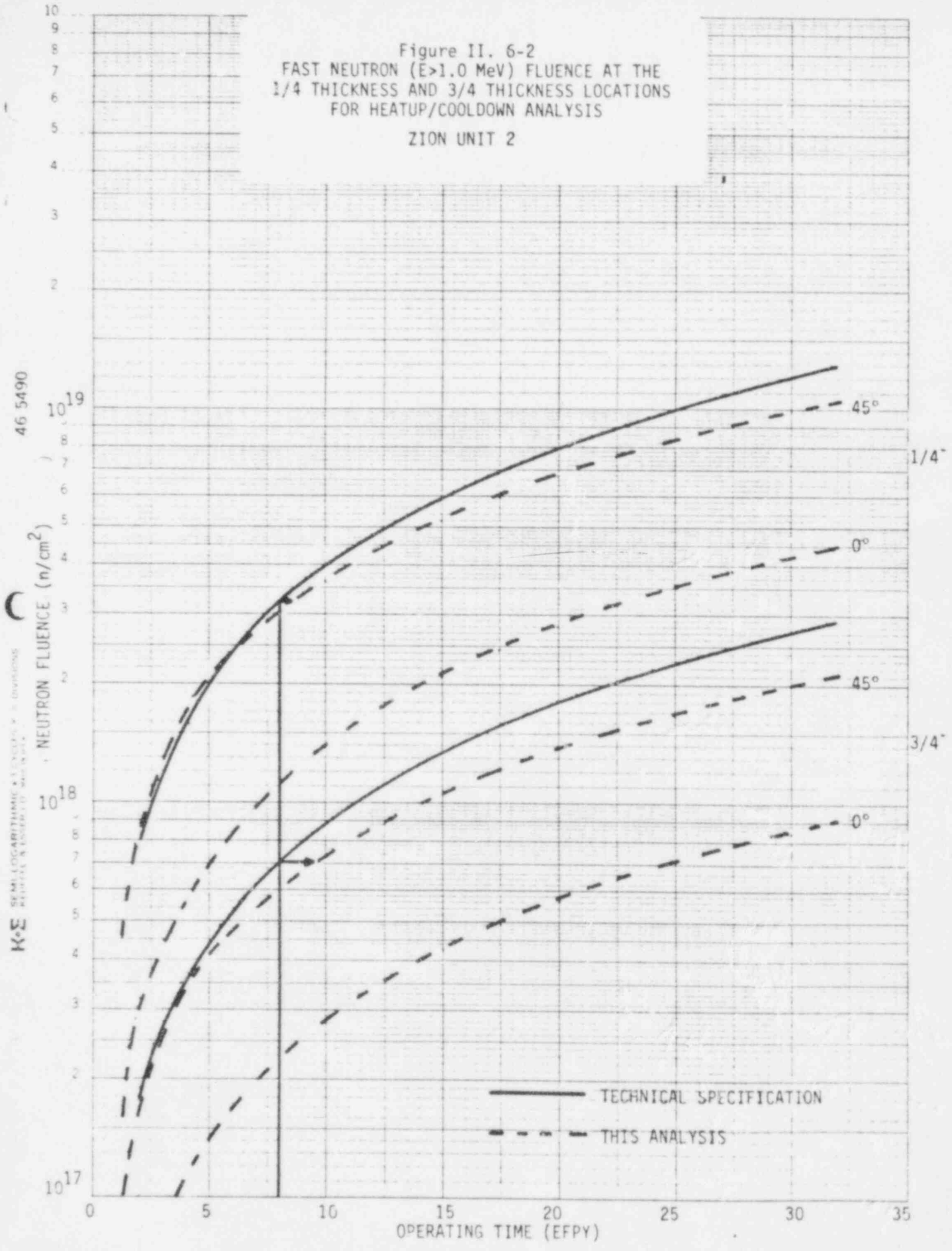

46 5490

K·E SEMI-LOGARITHMIC

SECTION III

SUMMARY AND CONCLUSIONS

Detailed fast neutron exposure evaluations using plant specific cycle by cycle core power distributions and state-of-the-art neutron transport methodology have been completed for the Zion Units 1 and 2 pressure vessels and surveillance capsules. Explicit calculations were performed for the first seven operating cycles of both units. For both units, projection of the fast neutron exposure beyond the current operating cycle was based on continued implementation of low leakage fuel management similar to that employed during cycle 7 for Unit 1 and cycles 6 and 7 for Unit 2.

In regard to the low leakage fuel management already in place at the Zion Units, the plant specific evaluations have demonstrated that for the low leakage case the average fast neutron flux at the 45° azimuthal position has been reduced by about 35% at Unit 1 and 25% at Unit 2 relative to that existing prior to implementation of low leakage. In particular, the following data applies at the 45° location.

	ϕ (n/cm^2-Sec)	
	Unit 1	Unit 2
Out-In Pattern	2.51×10^{10}	2.42×10^{10}
Low Leakage Pattern	1.63×10^{10}	1.76×10^{10}

This location represents the maximum fast neutron flux incident on the reactor pressure vessel. At other locations on the vessel, as well as at the surveillance capsules, the impact of low leakage will differ from the data presented above.

It should be noted that significant deviations from the low leakage scheme already in place will effect the exposure projections beyond the current operating cycle. A move toward a more severe form of low leakage (lower

relative power on the periphery) would tend to reduce the projection. On the other hand, a relaxation of the loading pattern toward higher relative power on the core periphery would increase the projections beyond those reported. As each future fuel cycle evolves, the loading patterns should be analyzed to determine their potential impact on vessel and capsule exposure.

Implementation of low leakage loading also effects the magnitude of the neutron flux at the surveillance capsule locations as well as the lead factors relating capsule exposure to maximum vessel exposure. Therefore, the assumptions of constant lead factors and capsule exposure rates over plant lifetime are not necessarily valid. Data depicting actual capsule exposure as a function of full power operating time has been presented in this report for both Zion Units. It is recommended that capsule withdrawal schedules be adjusted based on this plant specific information. Again, the potential impact of future changes in fuel management strategy should also be factored into any rescheduling of capsule withdrawals.

The fast neutron fluence values from the plant specific calculations have been compared directly with measured fluence levels derived from neutron dosimetry contained in three surveillance capsules withdrawn from each of the Zion Units. For Unit 1, the ratio of calculated to measured fluence values ranges from 0.93 to 1.02 for the three capsule data points. The corresponding ratio for Unit 2 is 0.95 for both capsules removed from that reactor. This excellent agreement between calculation and measurement supports the use of this analytical approach to perform plant specific evaluation for the Zion reactors.

The fuel management strategies employed to date essentially have had no impact on the schedule of applicability, i.e., 8 EFPY, for the heatup and cooldown pressure-temperature limit curves in the Zion Unit 1 and 2 technical specifications used for plant operation.

SECTION IV

REFERENCES

1. Soltesz, R. G., Disney, R. K., Jedruch, J. and Ziegler, S. L., "Nuclear Rocket Shielding Methods, Modification, Updating and Input Data Preparation Vol. 5 - Two Dimensional, Discrete Ordinates Transport Technique," WANL-PR(LL)034, Vol. 5, August 1970.

2. "Sailor RSIC Data Library Collection DLC-76," Coupled, Self-Shielded, 47 Neutron, 20 Gamma-Ray, P_3, Cross Section Library for Light Water Reactors.

3. Benchmark Testing of Westinghouse Neutron Transport Analysis Methodology - to be published.

4. Letter MMT-SME-915, "Heatup and Cooldown Curves for Zion Units I (CWE) and II (COM) based on a Longitudinal Flaw in the Circumferential Weld," April 30, 1979.

5. Letter MMT-SME-936, "Heatup and Cooldown Curves for Zion Units I (CWE) and II (COM) based on Surveillance Capsule Data," May 10, 1979.

6. "Effects of Residual Elements on Predicted Radiation Damage to Reactor Vessel Materials," Regulatory Guide 1.99 - Revision 1, U.S. Nuclear Regulatory Commission, Washington, April 1977.

7. Zion Technical Specification; Figure 3.3.2-1 (Heatup) and Figure 3.3.2-2 (Cooldown); Amendment 50 - Unit 1, Amendment 47 - Unit 2.

8. Commonwealth Edison letter from D. E. O'Brien to Mr. Albert Schwencer (NRC), "Zion Station Units 1 and 2 NRC Docket Nos. 50-295 and 50-304," September 7, 1977.

APPENDIX A

POWER DISTRIBUTIONS

Core power distributions used in the plant specific fast neutron exposure analysis of the Zion Units 1 and 2 pressure vessels were derived from the following fuel cycle design reports and verified by comparison with burnup data supplied by Commonwealth Edison [8].

Fuel Cycle	Unit 1	Unit 2
1	WCAP-7675-R1	WCAP-7675
2	WCAP-8616	WCAP-8881
3	WCAP-9114	WCAP-9246
4	WCAP-9356	WCAP-9458
5	WCAP-9568	WCAP-9687
6	WCAP-9859	WCAP-9959
7	WCAP-10047	WCAP-10282

A schematic diagram of the core configuration applicable to Zion Units 1 and 2 is shown in Figure A.1-1. Cycle averaged relative assembly powers for each operating fuel cycle of Zion Units 1 and 2 are listed in Tables A.1-1 and A.1-2, respectively.

On Figure A.1-1 and in Tables A.1-1 and A.1-2 an identification number is assigned to each fuel assembly location; and three regions consisting of subsets of fuel assemblies are defined. In performing the adjoint evaluations, the relative power in assemblies comprising Region 3 has been adjusted to account for known biases in the prediction of power in the peripheral assemblies while the relative power in assemblies comprising Region 2 has been maintained at the cycle average value. Due to the extreme self-shielding of the reactor core neutrons born in fuel assemblies comprising Region 1 do not contribute significantly to the neutron exposure either at the

Figure A.1-1

Zion Units 1 and 2 Core Description
for Power Distribution Maps

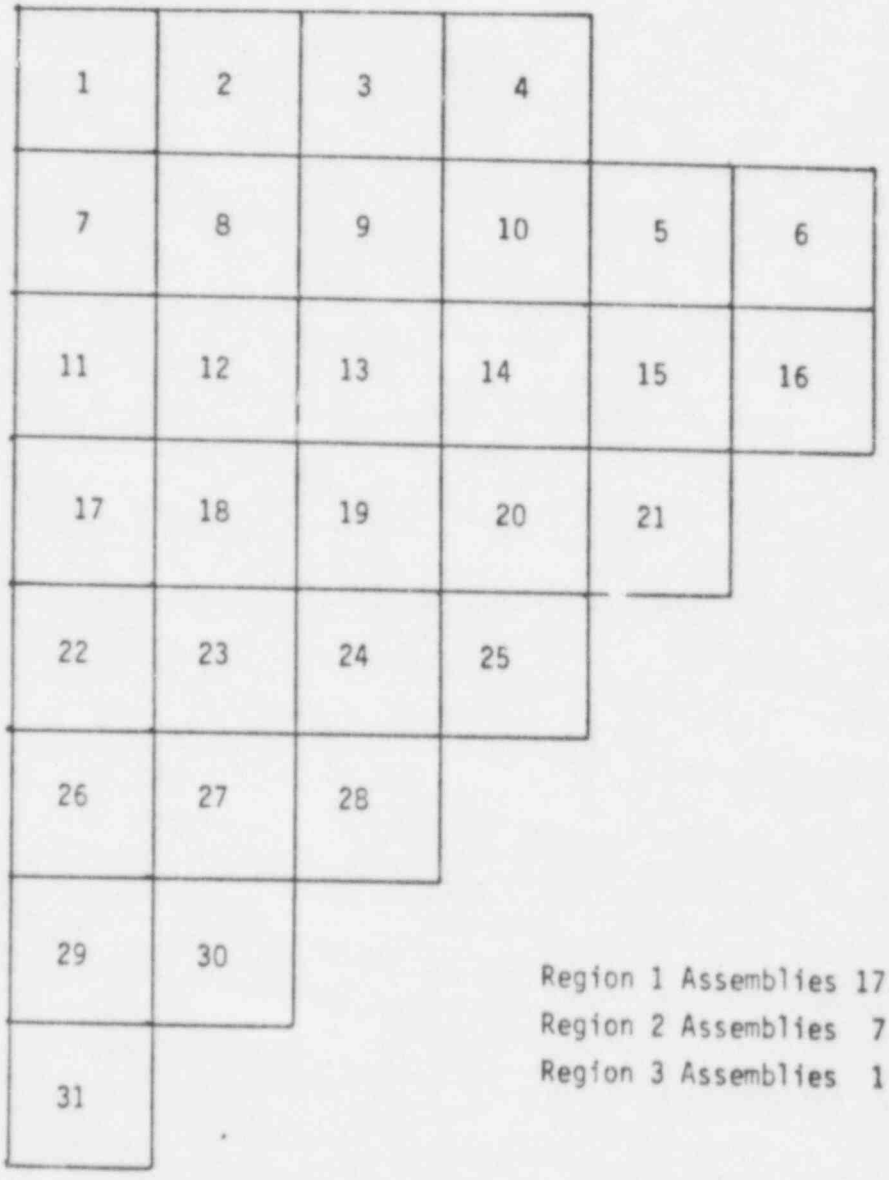

Region 1 Assemblies 17 - 31
Region 2 Assemblies 7 - 16
Region 3 Assemblies 1 - 6

TABLE A.1-1

CORE POWER DISTRIBUTIONS USED IN THE PLANT SPECIFIC FLUENCE ANALYSIS

ZION UNIT 1

	Fuel Cycle						
Assembly	1	2	3	4	5	6	7
1	0.81	0.98	0.98	0.91	1.02	0.96	1.00
2	0.89	0.98	1.01	0.95	1.01	0.99	1.03
3	0.76	0.92	0.95	0.89	1.01	1.01	0.95
4	0.66	0.73	0.75	0.73	0.86	0.80	0.47
5	0.93	0.99	1.03	1.06	1.10	1.10	0.64
6	0.56	0.63	0.71	0.71	0.74	0.77	0.39
7	1.04	0.97	0.87	0.83	0.92	0.88	0.79
8	1.05	1.16	1.23	1.17	1.16	0.91	1.13
9	1.01	0.96	0.99	0.96	1.01	1.19	1.13
10	1.02	1.18	1.14	1.16	1.19	1.11	1.05
11	1.17	0.94	0.82	0.86	0.82	1.08	0.89
12	1.12	0.95	0.87	0.89	0.92	1.15	1.01
13	1.15	0.95	0.93	0.90	1.29	1.13	1.23
14	1.08	1.11	1.19	1.01	1.02	1.02	1.08
15	0.97	0.99	0.99	1.19	1.08	1.16	1.13
16	1.04	0.90	1.12	1.01	0.84	0.99	1.04

TABLE A.1-2

CORE POWER DISTRIBUTIONS USED IN THE PLANT SPECIFIC FLUENCE ANALYSIS

ZION UNIT 2

Assembly	Fuel Cycle 1	2	3	4	5	6	7
1	0.80	1.04	0.89	0.59	0.95	0.88	0.72
2	0.87	1.05	0.92	0.81	0.95	0.99	0.92
3	0.75	0.98	0.85	0.83	0.90	0.91	0.85
4	0.65	0.77	0.68	0.70	0.70	0.47	0.46
5	0.92	0.99	0.98	1.01	0.98	0.91	0.96
6	0.53	0.64	0.67	0.73	0.72	0.41	0.43
7	1.02	0.96	0.87	0.77	0.88	0.89	1.19
8	1.03	1.20	1.18	1.16	1.11	1.12	1.17
9	1.00	0.98	0.94	0.92	0.89	1.16	0.90
10	1.00	1.20	1.14	1.14	1.05	1.09	1.12
11	1.17	0.87	0.93	0.98	1.05	1.09	1.21
12	1.12	1.03	1.00	0.98	0.97	0.99	1.07
13	1.15	0.94	1.10	1.01	1.19	1.18	1.24
14	1.08	0.96	1.12	0.97	0.92	1.15	1.01
15	0.97	0.88	1.01	1.03	0.88	0.91	1.04
16	1.02	0.87	1.06	1.16	1.11	0.97	1.05

surveillance capsules or at the pressure vessel. Therefore, power distribution data for assemblies in Region 1 are not listed in Tables A.1-1 and A.1-2.

In each of the adjoint evaluations, within assembly spatial gradients have been superimposed on the average assembly power levels. For the peripheral assemblies (Region 3), these spatial gradients also include adjustments to account for analytical deficiencies that tend to occur near the boundaries of the core region.